Photoelectrochemical etching of ZnSe and nonuniform charge flow in Schottky barriers

R. Tenne and H. Flaisher

Department of Plastics Research, The Weizmann Institute of Science, Rehovot 76100, Israel

R. Triboulet

*Laboratoire de Physique des Solides du Centre National de la Recherche Scientifique,
1 place A. Briand, F-92190 Meudon-Bellevue, France*

Photoelectrochemical etching of ZnSe, similar to that which was employed for cadmium chalcogenides, is found to decrease electron-hole recombinations upon photoexcitation considerably and to change the morphology of the semiconductor surface. Thus the photocurrent of a single-crystal ZnSe electrode in various electrolytes increases considerably (up to 100%) after such treatment. A unique morphology consisting of a dense pattern (10^9 cm^{-2}) of etch pits is revealed after photoetching. This pattern is believed to reflect the dopant distribution close to the surface. Onset potential measurements show an anodic shift in the flat-band potential after photoetching which may arise from reduced pinning of the Fermi level associated with elimination of surface states. These measurements also indicate that the average dopant density close to the semiconductor surface is reduced after photoetching in accordance with our model of nonuniform hole flow in the space-charge region.

I. INTRODUCTION

ZnSe is a large-band-gap semiconductor ($E_g = 2.7$ eV) which is used as a window in high-power, infrared lasers and as a blue-light light-emitting diode (LED) device. It has a zinc-blende structure at room temperature and its solid-state properties were investigated in the past by a number of workers. An early study of ZnSe in electrochemical cells was reported.[1] ZnSe-based photoelectrochemical cells were investigated recently by Gautron et al., who characterized the solid-state properties of ZnSe in various electrolytes[2] using such techniques as photocurrent spectroscopy, capacitance measurements, and electrolyte electroreflectance.

Photoelectrochemical etching was found to improve the state of the surface of various semiconductors.[3] I-V measurements combined with electron microscopy,[3(b)] spectral response measurements,[4] electroluminescence,[5] electron-beam-induced current[6] (EBIC), and cathodoluminescence[7] gave strong evidence that surface defects which are not accessible to any chemical etchant are selectively (or preferentially) etched out of the surface of cadmium-chalcogenide semiconductors using this technique. The physical and the chemical nature of these defects is not yet fully understood. A recent study[8] suggests that the unique morphology of photoetched cadmium-chalcogenide semiconductors can be attributed to the dopant distribution, and therefore it is possible that at least some of the defects on the semiconductor surface might be associated with lattice imperfections introduced by the dopant atom. Selective photoelectrochemical etching has been successfully applied also for ternary materials such as CdIn$_2$X$_4$ ($X=$S,Se).[9,10] Electrolyte electroreflectance measurements showed that surface defects are preferentially etched from the surface of CdIn$_2$Se$_4$ upon a short photoetch.[11] It was also demonstrated that the state of the

surface of p-type semiconductors (e.g., p-type CdTe) can be improved using selective electrochemical etching (no light was necessary here).[12]

In the present work, we want to report on the photoelectrochemical etching of ZnSe (n type) and on the remarkable effect it has on the performance of a ZnSe photoelectrochemical cell and on the morphology of the surface of that material. The ZnSe photoelectrode was tested in various electrolytes and in all of them, considerable improvements in the photocurrent were obtained after photoetching. A sulfite (SO$_3^{2-}$) solution was preferred for most of our measurements since it is transparent to the exciting light, and since the rate of photocorrosion of ZnSe is relatively slow in this electrolyte.

II. EXPERIMENTAL

ZnSe crystals were grown by the iodine transport method and were annealed in a Zn atmosphere at 700 °C.[13] The dopant density was found to be on the order of $(4-5)\times 10^{17}$ cm^{-3}. The crystal was first polished using alumina paste (Buehler, 0.3 μm grit) and then etched in a mixture of three parts H$_2$SO$_4$ and seven parts saturated K$_2$Cr$_2$O$_7$ solution. Ohmic contact was established by smearing an In-Ga alloy (melting point 70 °C) on the back surface of the electrode. Conductive silver epoxy (Transene 50) was used to attach the crystal to a Ti plate, and finally, the electrode was insulated apart from its front surface by applying an insulating epoxy. Various solutions were tested for both the chemical etching and photoetching of the semiconductor surface. They included: (1) a solution consisting of one part HNO$_3$, four parts HCl (aqua regia); (2) a mixture of three parts H$_2$SO$_4$, seven parts saturated K$_2$Cr$_2$O$_7$ solution; (3) a solution containing 4 g K$_2$Cr$_2$O$_7$, 10 ml HNO$_3$, and 20 ml water; (4) a solution of 6 g CrO$_3$, 4 g H$_2$O, and 10 g HCl, and finally, (5) 2%

Br_2 in 98% methanol.

The photoetching was successfully performed in the first-three solutions which were diluted 5—10 times to prevent competition between the photoetching and the chemical etching. The semiconductor was exposed to a reverse bias of over 1 V accompanied by high-intensity illumination in order to enhance the selectivity of the process.[3(d)] The duration of the photoetching usually did not exceed 5 sec. Afterwards, the electrode was rinsed and immersed in a concentrated polysulfide solution to dissolve any elemental selenium from the electrode surface. The photoetching process was repeated 2—3 times until no improvement in the stabilized photocurrent was observed. A stabilized tungsten iodine lamp which delivered greater than 2 AM1 light intensity was employed throughout these experiments both for the photoetching process and in the measurement of I-V characteristics. A lock-in technique was used to obtain the action spectra and onset potential (Fig. 4) prior and after photoetching. Scanning electron microscopy (Jeol 35) was used to determine the morphology of the electrodes prior to and after photoetching.

The solutions which were used for the photoelectrochemical cells were the following: (1) $0.3M$ $Fe(CN)_6^{4-}$/ $0.1M$ $Fe(CN)_6^{3-}$; (2) $1M$ Na_2S/KOH solution, and (3) $1M$ Na_2SO_3 solution. They were prepared by dissolving the appropriate amount of salt in deionized water which was carefully deaerated with argon gas. The positive effect of

FIG. 1. Photocurrent vs potential curves for ZnSe in $1M$ Na_2SO_3 solution prior to and after photoetching. (a) Chromate etch (No. 2) prior to photoetch. (b) Br_2 (2%)—methanol (No. 5) etch.

the photoetching on the photocurrent of the cell was observed in all three solutions, but only the results obtained using the latter solution are reported here.

III. RESULTS

Figure 1 shows the I-V curve of a ZnSe electrode immersed in $1M$ sulfite (SO_3^{2-}) electrolyte both before and after photoetching. Two cases are shown for two different etching solutions. The photocurrent of the cell increased considerably in all cases, immaterial of the previous chemical etching treatment, the kind of solution used for the photoelectrochemical cell and the light intensity used in the I-V measurements. This shows that a short photoetching removes defects from the surface of the semiconductor which are normally not accessible to the chemical etchant. It is also significant to note that the improvement in the photocurrent under forward bias is even more substantial than under reverse bias. In general, the extent of hole recombinations due to surface defects is greater under forward bias as compared to reverse bias conditions. It has been shown in the past that removal of surface defects[3,8] or their passivation[14] have larger effect under forward bias than under reverse bias conditions.

The morphological changes of the semiconductor surface caused by photoetching are shown in Fig. 2, where we compare the scanning-electron-microscope image of (a) a chemically etched and (b) a photoetched ZnSe crystal. A dense pattern ($\sim 10^9$ cm^{-2}) of submicrometer etch pits appears on the surface of the photoetched electrode [Fig. 2(b)], similar to the one observed previously on the surface of photoetched cadmium-chalcogenide semiconductors. This kind of pattern was observed on different crystal faces of the semiconductor, and it was not sensitive to the photoetching time, bias, and light intensity within certain limits.

The morphology of the photoetched surfaces was also insensitive to the kind of chemical etchant which was previously employed, and it was also insensitive to the type of photoetching solution employed, provided a strong reverse bias and high light intensity were employed. It is also important to note that, in ZnSe, the dopants are intentionally introduced iodine atoms, whereas in the cadmium-chalcogenides, the dopants are the residual impurities Cu, Ag, Li, and P (p type) and Al or In (n type).[15] This shows that the selectivity of the photoetching process and its unique effect on surface morphology depend on the *presence* of dopant centers and not on their chemical nature.

Figure 3 shows the spectral response on ZnSe prior to and after photoetching. Although no subband gap was observed prior to the photoetching, the somewhat more well-defined band gap (steeper increase of spectral response around 460 nm) suggests that the photoetching removed some unspecified surface defects. These defects increase the rate of electron-hole recombination on the semiconductor surface. Similar observations were found on photoetched materials of various kinds.[3(d),4,9,12] Another interesting property of the photoetched electrode is the red shift in the maximum of the spectral response in Fig. 3. This red shift, which was always observed after the photoetching, varied somewhat in magnitude from one
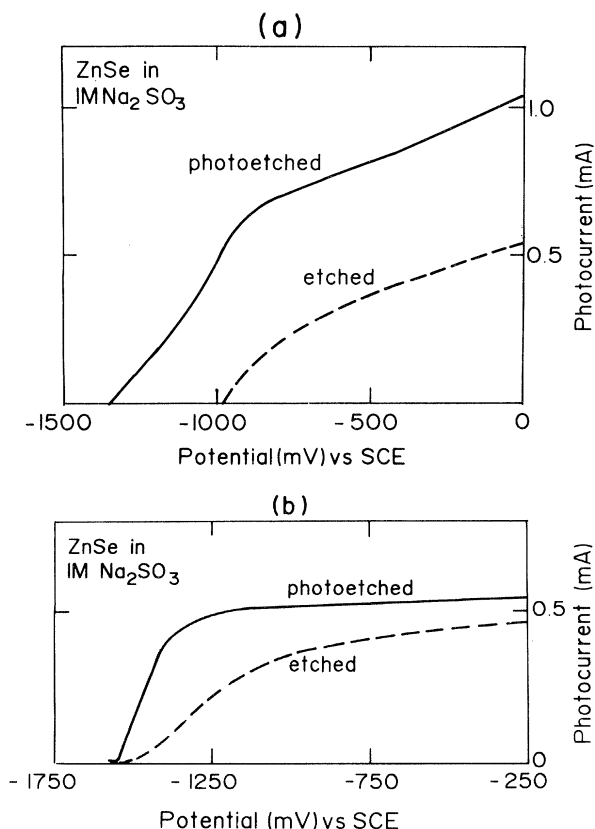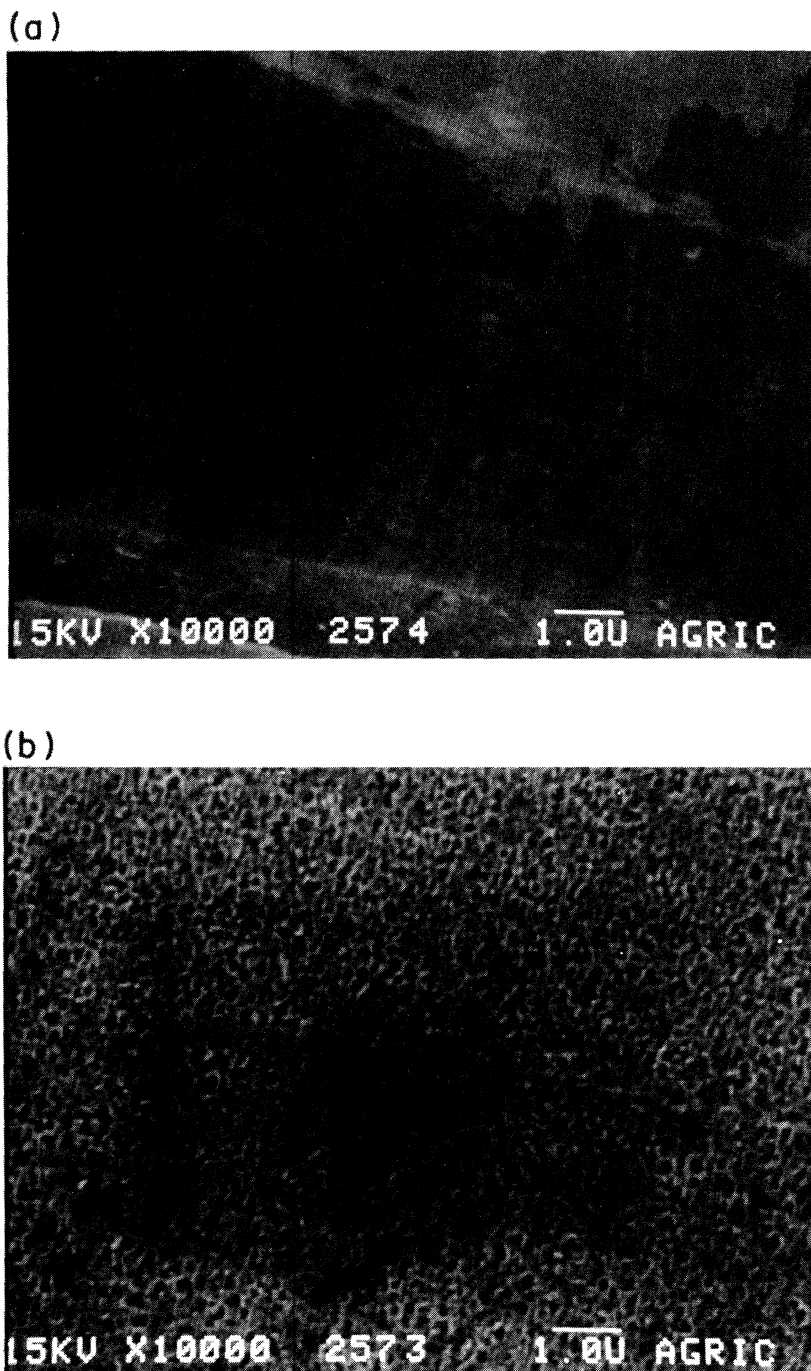
(a)

(b)

FIG. 2. Scanning electron-microscope images ($\times 10\,000$) for Br_2 (2%)—methanol (a) etched and (b) photoetched ZnSe electrode. Note the similarity between the morphology of photoetched ZnSe and photoetched cadmium-chalcogenide semiconductors (Refs. 3 and 8).

experiment to the other, and it is discussed in detail in the following section.

It has been shown here that a short photoetching of ZnSe photoelectrodes leads to a substantial improvement in their photocurrent due to a reduced surface recombination velocity. The morphology of photoetched ZnSe resembles that of cadmium-chalcogenide electrodes where a high density of etch pits (10^9–10^{10} cm^{-2}) was found after photoetching.

To determine the flat-band potential we used a lock-in technique and plotted the square of the photocurrent versus the electrode potential.[2(a)] These results are presented in Fig. 4 (the "experimental" points are obtained by fitting a curve to the experimental data which was
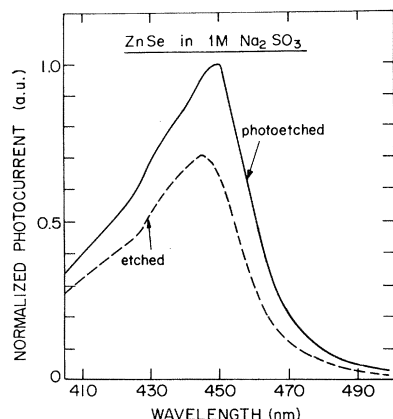
FIG. 3. Spectral reponse of ZnSe prior to and after photoetching. Note the red shift in the maximum of the response curve for the photoetched electrode.

noisy due to hydrogen evolution). Mott-Schottky plots indicated a similar flat-band potential for this system.

IV. DISCUSSION

The two salient features of the onset voltage plot of Fig. 4 are the anodic shift of the flat-band potential and the increased slope of the curve after photoetching. The first result may arise from a partial pinning of the semiconductor Fermi level to a distribution of surface states under strong forward bias. It is possible that the photoetching reduces the density of these states,[11] thereby leading to a reduction in pinning and an anodic shift in the flat-band potential.

In the linear approximation which is used to obtain Fig. 4, one can show that

$$\frac{dJ_{ph}^2}{dV} = (\alpha\phi)^2 \frac{2q\epsilon_s\epsilon_0}{N_D} , \qquad (1)$$

where J_{ph} is the photocurrent, V is the applied potential, α is the absorption coefficient, ϕ is the light flux, q is the elementary charge, ϵ_s is the dielectric constant, ϵ_0 is the permittivity of free space, and N_D is the doping density. Thus Eq. (1) suggests that the larger slope in the curve after photoetching may be connected with a reduced average doping density on the semiconductor surface.
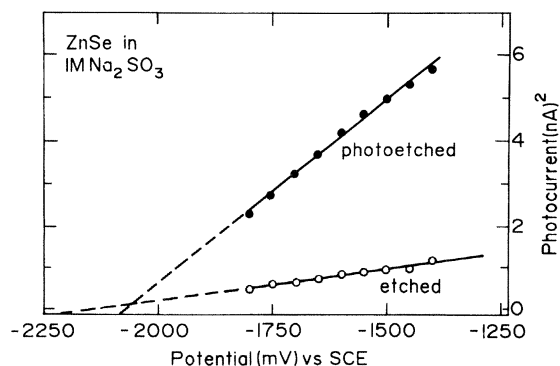
We have shown that photoelectrochemical etching improves the state of the ZnSe surface leading to higher photocurrents and reduced electron-hole recombination. The etch-pit pattern seems to be connected with the dopant distribution close (< 100 Å) to the semiconductor surface. In order to explain this we use Fig. 5. Here, a cross section of the solid-electrolyte interface is schematically represented. The ionized donors in the space-charge layer of a semiconductor (n type) are not neutralized by the charge of the electron cloud which exists in the bulk of the semiconductor. Since these ionized donors are localized, they induce a strong electric field in their immediate proximity. Looking from outside the interface there is no electric field in the interfacial (y-z) plane, and there is a monotonically decreasing electric field (the space-charge field) in the coordinate (x) perpendicular to the interface. The overall thermodynamics and the kinetics of charge transfer are determined by the macroscopic field, but the particular trajectory of each charge carrier is determined to some extent also by the local electrical fields induced by each donor ion. As a result of these local fields the current flow of the minority (and majority) carriers is nonuniform. This nonuniformity can be manifested in two ways. First, the perpendicular (x-direction) component of the electric field is strongest wherever there is a donor ion close to the surface (dopant zone). This leads to a higher collection efficiency of photogenerated holes in the dopant zones so that the rate of the photoetching in these regions is higher than outside these zones. Consequently, the dopant atoms are selectively removed from the semiconductor surface after photoetching. On the other hand, holes which are created behind the outermost layer of dopant ions drift toward the surface in a trajectory of minimum potential energy, i.e., between the dopant zones. However, since more photons are absorbed in the outermost layer of the crystal than deep in the bulk of the semiconductor, it is expected that the doping density of the semiconductor is lowered after photoetching, according to the former mechanism.

Using the Gärtner model[16] and assuming a direct band gap with the absorption coefficient α varying as

$$\alpha = A \frac{(h\nu - E_g)^{1/2}}{h\nu} , \qquad (2)$$

FIG. 4. Determination of flat-band potential from onset potential measurements, $\lambda = 480$ nm. (SCE denotes saturated calomel electrode.)
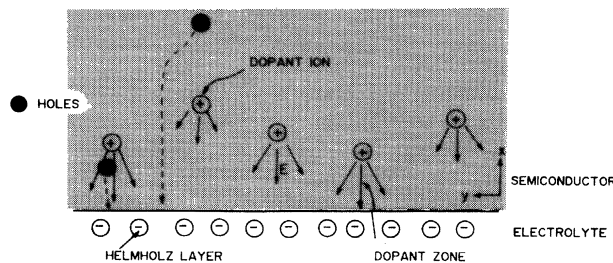

FIG. 5. Schematic representation of the interface between an n-type semiconductor and electrolyte which creates a Schottky barrier. The arrows represent the local electric field included by the ionized (and non-neutralized) donors $\oplus$ and the conductive electrolyte (metal) phase. ● are photogenerated holes and the dashed arrows represent their trajectory in the local fields induced by the donors and the space-charge field (x direction).
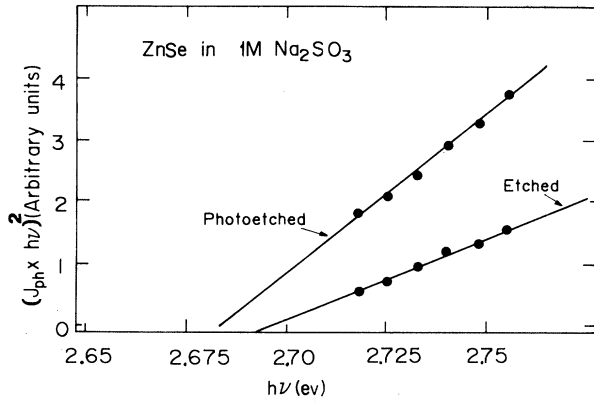
FIG. 6. Determination of the absorption edge (effective band gap) prior to and after photoetching. The difference in the effective band gap agrees with the Burstein-Moss model for heavily doped semiconductors (see text).

where E_g is the band gap, $h\nu$ is the photon energy, and A is the a constant, one can write the photocurrent as

$$i_{ph} = C\frac{(h\nu - E_g)^{1/2}}{h\nu} \qquad (3)$$

in the linear approximation (i.e., αW, $\alpha Lp \ll 1$, where W is the width of the space-charge layer and Lp is the hole diffusion length).

Figure 6 shows the plot of $(i_{ph}h\nu)^2$ vs $h\nu$ as obtained using a lock-in technique. The extrapolation to zero gives the band gap of ZnSe prior to (2.695 eV) and after (2.683 eV) photoetching.

One possible explanation to the red shift in the band gap after photoetching is given by the Burstein-Moss model for heavily doped semiconductors. According to this model, excitation of electrons by photons of energy $h\nu = E_g$ is not possible in heavily doped semiconductors, since the lower-energy states in the conduction band are fully occupied, and only states with higher energy are permissible.

Using an effective mass of the electrons in the conduction band (m_e^*) as $0.17m_e$,[17] where m_e is the electron mass, we calculate the density of states in the conduction band to be, in units of cm^{-3},

$$N_C = 1.75 \times 10^{18} . \qquad (4)$$

Since the doping density of the studied sample is $(4-5) \times 10^{17}$ cm^{-3}, it is possible that a Burstein-Moss shift due to reduced doping of the semiconductor surface occurs after photoetching. By considering this to be the case, the shift in the band-gap energy (ΔE) is given by[18-20]

$$\Delta E = (h^2/8m_e^*)(3N_D/\pi)^2 . \qquad (5)$$

Using the experimental shift in the band gap $(12m_e V)$ and the effective mass of the electron $m_e^* = 0.17m_e$,[17] we obtain a value, in units of cm^{-3}, of

$$N_D = 4.1 \times 10^{17} , \qquad (6)$$

in very good agreement with the donor density as determined from Hall-effect measurements.

Alternatively, one can explain the observed red shift in the photocurrent spectrum from the dependence of excitonic transitions on the doping density.[17(a),21-24] Appreciable red shifts in the spectral response were found after photoetching of various materials.[9,25] The simple Burstein-Moss equation [Eq. (5)] is not applicable in some cases, since this equation assumes that the material has a spherical Fermi surface.

We would now like to correlate the doping density to the etch-pit density. The width of the space-charge layer is given by

$$W = (2\epsilon_0\epsilon_s/qN_D)^{1/2}(V - V_{FB})^{1/2} , \qquad (7)$$

where V is the bias, V_{FB} is the flat-band bias, ϵ_0 is the permittivity of free space, and ϵ_s is the static dielectric constant [$\epsilon_s = 8.7$ (Refs. 17 and 21)]. Assuming a band bending of 1 V (equal to $V - V_{FB}$) during the photoetching, one obtains a value of 4.36×10^{-6} cm^{-3} for W. Multiplying that number by the donor density in Eq. (6), one finds that the number of ionized donors in the space-charge layer during the photoetching is about 1.79×10^{12} cm^{-2}. This number exceeds the surfacial density of etch pits $(10^9-10^{10}$ cm$^{-2})$ by more than 2 orders of magnitude. It is possible that the distribution of etch pits reflects the dopant distribution at the outermost layer of dopants as represented in Fig. 5. Other explanations for the above discrepancy, such as clustering of donors, or the validity of the simple law for the potential distribution in the space-charge layer [Eq. (7)], which in fact is questioned by the present work, cannot be excluded.

V. CONCLUSIONS

Quick photoetching of ZnSe leads to a significant reduction in electron-hole recombination on the semiconductor surface. A typical pattern of dense etch pits $(10^9-10^{10}$ cm$^{-2})$ appears on the semiconductor surface, and a red shift is observed in the spectral response curve after photoetching, which is explained by both the Burstein-Moss model for heavily doped semiconductors and by explanations involving the excitonic transition.

We have advanced the supposed mechanism for photoetching at the semiconductor surface. This mechanism involves the inherent nonuniformity of the electric field in the depletion layer, a subtle fact which is usually neglected in the literature concerning either p-n junctions or Schottky barriers. This concept of nonuniform charge flow in the plane perpendicular to the flow is, of course, relevant both for minority and majority carriers.

Finally, the fact that photoetching substantially improves the efficiency of charge transfer for zinc selenide, as it does for so many other types of semiconductors, proves once again that this is a necessary step in the preparation of efficient photoelectrochemical cells.

[1]R. Williams, J. Electrochem. Soc. 114, 1173 (1967).

[2](a) J. Gautron, P. Lemasson, F. Rabago and R. Triboulet, J. Electrochem. Soc. 126, 1868 (1979); (b) J. Gautron, C. Raisin, and P. Lemasson, J. Phys. D 15, 153 (1982), and references therein.

[3](a) G. Hodes, Nature 285, 29 (1980); (b) R. Tenne and G. Hodes, Appl. Phys. Lett. 37, 428 (1980); (c) R. Tenne, Appl. Phys. 25, 13 (1981); (d) N. Müller and R. Tenne, Appl. Phys. Lett. 39, 283 (1981).

[4]Y. Mirovsky, R. Tenne, G. Hodes, and D. Cahen, Thin Solid Films 91, 349 (1982).

[5]H. H. Streckert, J. Tong, and A. B. Ellis, J. Am. Chem. Soc. 104, 581 (1982).

[6]G. Hodes, D. Cahen, and H. Leamy, J. Appl. Phys. 54, 4676 (1983).

[7]R. Tenne and A. K. Chin, Mater. Lett. 2, 143 (1983).

[8]R. Tenne and G. Hodes, Surf. Sci. 135, 453 (1983).

[9]R. Tenne, Y. Mirovsky, Y. Greenstein, and D. Cahen, J. Electrochem. Soc. 129, 1506 (1982).

[10]G. F. Epps and R. S. Becker, J. Electrochem. Soc. 129, 2628 (1982).

[11]M. Tomkiewicz, W. Siripala, and R. Tenne, J. Electrochem. Soc. (in press).

[12]R. Tenne, Appl. Phys. Lett. 43, 201 (1983).

[13]R. Triboulet, F. Rabago, R. Legros, H. Lozykowski, and G. Aidier, J. Cryst. Growth 59, 172 (1982).

[14]A. Heller, Acc. Chem. Res. 14, 154 (1981).

[15]J. L. Pautrat, N. Magnea, and J. P. Faurie, J. Appl. Phys. 53, 8668 (1982).

[16]M. A. Butler, J. Appl. Phys. 48, 1914 (1977).

[17](a) G. E. Hite, D. T. F. Marple, M. Even, and B. Segall, Phys. Rev. 156, 850 (1967); (b) Data sheet supplied by Cleveland Crystals Inc.

[18]H. Jäger and E. Seipp, J. Appl. Phys. 52, 425 (1981).

[19]E. Burstein, Phys. Rev. 93, 632 (1954).

[20]T. S. Moss, Proc. Phys. Soc. London, Sec. B 67, 775 (1954).

[21]P. Lemasson, J. P. Dalbera, and J. Gautron, J. Appl. Phys. 52, 6296 (1981).

[22]P. Lemasson, Solid State Commun. 43, 627 (1982).

[23]H. Kukimoto, S. Shionoya, S. Toyotomi, and K. Morigaki, J. Phys. Soc. Jpn. 28, (1), 110 (1970).

[24]J. P. Löwenau, S. Schnitt-Rink, and H. Hang, Phys. Rev. Lett. 49, 1511 (1982).

[25]M. Ulmann and J. Augustynski, in Photoelectrochemistry: Fundamental Processes and Measurement Techniques, The Electrochemical Society Series, edited by W. L. Wallace et al. (Electrochemical Society, New York, 1982), Vols. 82 and 83, p. 663.
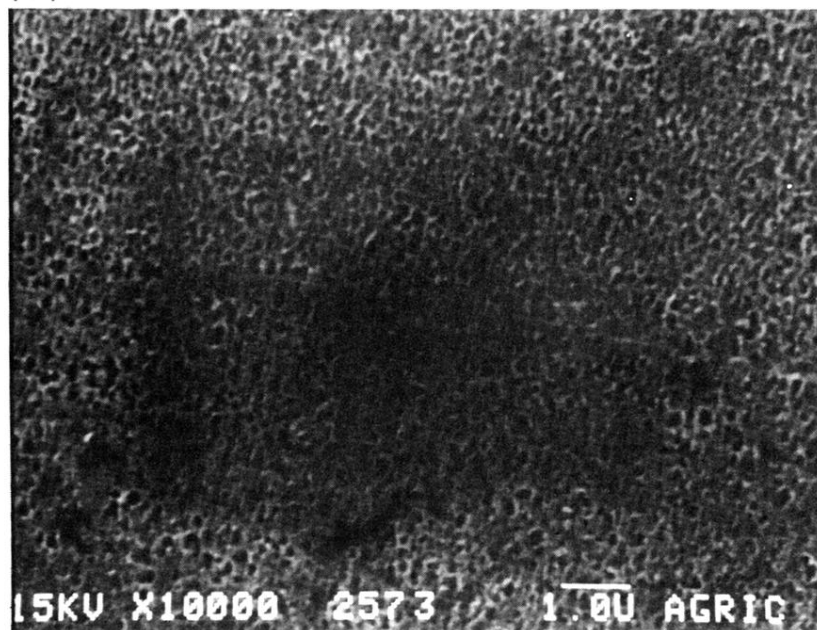
FIG. 2. Scanning electron-microscope images ($\times 10\,000$) for Br_2 (2%)—methanol (a) etched and (b) photoetched ZnSe electrode. Note the similarity between the morphology of photoetched ZnSe and photoetched cadmium-chalcogenide semiconductors (Refs. 3 and 8).
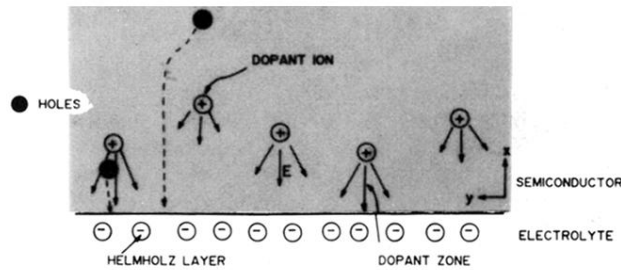
FIG. 5. Schematic representation of the interface between an n-type semiconductor and electrolyte which creates a Schottky barrier. The arrows represent the local electric field included by the ionized (and non-neutralized) donors $\oplus$ and the conductive electrolyte (metal) phase. $\bullet$ are photogenerated holes and the dashed arrows represent their trajectory in the local fields induced by the donors and the space-charge field (x direction).